Nucleon polarization in three-body models of polarized ^{6}Li

N. W. Schellingerhout* and L. P. Kok
Institute for Theoretical Physics, University of Groningen, Nijenborgh 4, NL-9747 AG Groningen, The Netherlands

S. A. Coon
Department of Physics, New Mexico State University, Las Cruces, New Mexico 88003

R. M. Adam†
Department of Physics and Astronomy, Vrije Universiteit, De Boelelaan 1081, NL-1081 HV Amsterdam, The Netherlands
(Received 3 June 1993)

Just as $^3\vec{\text{He}}$ can be approximately characterized as a polarized neutron target, polarized ^{6}LiD has been advocated as a good *isoscalar* nuclear target for the extraction of the polarized gluon content of the nucleon. The original argument rests upon a presumed "alpha + deuteron" picture of ^{6}Li, with the polarization of the nucleus carried by the polarization of the deuteron. We have calculated the polarization of the constituents of ^{6}Li as a three-body bound state of $\alpha + n + p$ interacting with local potentials fitted to the scattering data. It is necessary to include partial waves up to $j = \frac{17}{2}$ (75 channels, or, when including the $T = 1$ state, 150 channels) in the Faddeev equations before the energy eigenvalue converges. The longitudinal form factors are then described well by the wave function. Various combinations of αN and NN strong and Coulomb potentials yield a straight line in the charge radius vs. energy plane which, unlike those of previous calculations, passes through the experimental datum. We find for all cases a polarization of the valence neutron in excess of 90%. This may make polarized ^{6}LiD an attractive target for many nuclear physics purposes, since its neutrons are effectively 45% polarized.

PACS number(s): 21.45.+v, 24.70.+s, 11.80.Jy, 24.85.+p

I. INTRODUCTION

Targets of polarized nuclei are rather rare, so the recently acquired ability to produce a large solid target of polarized ^{6}LiD [1] has aroused much interest in the medium-energy and high-energy communities. In particular, this target has been suggested for measurements of direct photon production at Fermilab [2], and at the UNK proton accelerator under construction at Serpukhov. The cross section for direct photon production is dominated by the "Compton-like" subprocess "quark + gluon → gamma + quark." When both beam and target nucleons are longitudinally polarized, asymmetries in this process can be used to determine the polarized gluon distribution in a nucleon. Knowledge of this spin-dependent (polarized) gluon distribution is needed to extract the true spin-dependent quark and antiquark distributions from the deep-inelastic lepton-scattering data [3,4], and establish the relationship of the polarization of a nucleon to that of its quark and gluon constituents. For that particular high-energy experiment, the most sensitive experimental method would be to use a polarized isoscalar nucleon target, e.g., one made up of equal numbers of polarized protons and neutrons [5]. Polarized ^{6}LiD has been advocated as a good isoscalar nucleon target since "To the extent that $^6\vec{\text{Li}}$ can be viewed as He + $\vec{\text{D}}$, as much as one-half of the nucleons are polarized in such a material" [2]. (This is important from an experimental viewpoint because, by contrast, conventional polarized-proton-target materials contain less than 20% free hydrogen by weight.) One can ask the question "To what extent, indeed, is this true?" One of the goals of this paper is to provide a theoretical analysis and prediction of the polarization of the constituents of $^6\vec{\text{Li}}$ in a dynamical three-body model of ^{6}Li. In this picture ^{6}Li is a bound system of an alpha particle, a neutron, and a proton interacting with potentials which parametrize the free-space forces between the three "elementary" particles. We find that the optimistic polarization estimates of the high-energy physicists are fully justified in this more sophisticated (and realistic) model. We note, however, that the interest in the polarization of constituents of $^6\vec{\text{Li}}$ is not limited to this one investigation in high-energy physics, but indeed opens up possibilities of a variety of experimental and theoretical investigations of the spin structure of $^6\vec{\text{Li}}$. Some of these will be discussed in the closing section of this paper.

But is the three-body model of ^{6}Li truly realistic? The accumulating evidence from the confrontation of calculations with experiment answers this question with an emphatic yes. Many properties of the trio of $A = 6$ nuclei at low excitation energies ($\leq$ 15 MeV) can be understood within the context of exact three-body theory and good

*Electronic address: schellin@th.rug.nl
†Present address: Department of Physics, University of South Africa, P.O. Box 392, Pretoria, 0001, South Africa.

phenomenological representations of the low energy (below 23 MeV) behavior of the basic interactions [6,7]. The quality of the predictions is better than that of effective two-cluster models or the standard shell model which reduces in its effect to two-body dynamics. As two recent examples of this claim, we cite predictions of the proton-knockout reaction ^{6}Li$(e,e'p)$ and of the quadrupole moment Q. The former reaction is well described below α breakup by a three-body model and cannot be described by a (small space) shell-model calculation [8]. According to Mertelmeier and Hofmann [9], the latter small negative value of Q cannot be reproduced in a cluster model by a pure (αD) wave function. Instead a modern resonating-group model needs a three-body (αnp) wave function with s and d partial waves between the clusters and within the "deuteron" to match experiment. This result corroborates the earlier conclusions of the Surrey group and others [10]. These predictive aspects of the three-body model are even more interesting once one realizes that, in contrast to the effective two-body models, once the parameters of the model are determined at the αN and NN level, no further parametrization is allowed and all the results obtained thereafter are direct predictions of the model.

In this paper we present solutions of the Faddeev equations for a number of three-body models of ^{6}Li which differ by various combinations of αN and NN potentials. For each model, we calculate the longitudinal charge form factors F_{C0} and F_{C2} and associated lowest moments (charge radius and quadrupole moment) to assess the static properties of the wave function. From the wave function we calculate the polarization of the neutron and the proton outside the α. We find for all cases a polarization of the neutron in excess of 90% of the polarization of the ^{6}Li nucleus, implying an effective neutron polarization in excess of 30%. This degree of polarization is not as high as the predicted 87% polarization of the neutron in a fully polarized ^{3}He target [11]. However, for some nuclear physics purposes, a *dense* (^{6}LiD is a solid), *isoscalar* ($T = 0$) polarized target with an effective neutron polarization of 45% (the polarization of the neutron in $\vec{\text{D}}$ is over 95%) may be an attractive alternative to obtaining polarized neutrons from a *gaseous*, $T = \frac{1}{2}$, $^3\vec{\text{He}}$ target.

We note already the first use of a polarized ^{6}Li target for nuclear research to obtain the angular distribution of the vector analyzing power iT_{11} for π^+-$^6\vec{\text{Li}}$ elastic and inelastic scattering [12]. We will discuss the interpretation of this experiment in a later section, but note for the moment that polarization predictions of models of ^{6}Li should be tested by knockout reactions [8,13], scattering by polarized proton beams [14], and other experimental probes. That is, a program for ^{6}Li similar to the program which tests the ^{3}He wave function by knockout reactions [15], scattering by polarized proton beams [16], etc., would, in our opinion, be helpful to test our predictions. This is, first, because the prediction is couched as the answer to the question "If we pick a nucleon from the fully polarized nucleus without disturbing its spin, what is the degree of polarization of that spin?" This question is a theorist's question and may or may not be answerable in a given experiment. For example, any spin-dependent final-state interactions or spin-dependent meson-exchange currents can alter the "plucked" nucleon's spin. Second, the answer is based on calculated wave-function probabilities (or, in the general case with isospin breaking, off-diagonal matrix elements) which are unambiguously obtained from the interaction operators. These quantities are not experimental observables, however, because of the problems of defining uniquely the relativistic corrections to the interaction operators [17,18]. Hence, experimental tests of our predictions are required. We hope that our predictions could be used to motivate such experiments.

This paper is organized as follows: Sec. II briefly sketches our solution to the Faddeev equations. We derive expressions for constituent polarization based on wave-function probabilities in Sec. III. After a brief description of the potentials which differentiate the models in Sec. IV, we discuss the different sources of uncertainty within the three-body model (by looking at binding energies, charge radii, quadrupole moments) in Sec. V. A comparison of observables with experiment and other theoretical calculations to establish the quality of the three-body model itself is given in Sec. VI. Our predictions for polarization of the valence nucleons and other aspects of wave-function probabilities are discussed in Sec. VII. We give a summary and outlook in Sec. VIII.

II. FORMALISM

We will be modeling ^{6}Li as a three-body cluster model, assuming the α particle to be structureless. The three-body problem will be solved by applying the spline method to the configuration-space Faddeev equations. The form of the Faddeev equations is well known and will simply be sketched here. We will, however, give some definitions which are essential to the understanding of the rest of this paper.

The Schrödinger equation for three particles interacting via two-body forces

$$(H_0 + V_1 + V_2 + V_3 - E)\Psi = 0\,, \tag{1}$$

where V_i is the interaction between particles j and k, and H_0 is the kinetic energy operator, is equivalent to the Faddeev equations

$$\begin{aligned}(E - H_0 - V_1)\psi_1 &= V_1(\psi_2 + \psi_3),\\ (E - H_0 - V_2)\psi_2 &= V_2(\psi_3 + \psi_1),\\ (E - H_0 - V_3)\psi_3 &= V_3(\psi_1 + \psi_2)\,,\end{aligned} \tag{2}$$

from which the total wave function can be constructed by addition of the Faddeev amplitudes ψ_i:

$$\Psi = \psi_1 + \psi_2 + \psi_3\,. \tag{3}$$

Another, sometimes useful, form of the Faddeev equations is

$$(E - H_0)\psi_i = V_i\Psi\,, \tag{4}$$

which follows immediately from Eq. (3).

By expanding the Faddeev amplitudes on a basis of angular-momentum eigenfunctions (also known as channels), the Faddeev equations can be rewritten as an infinite set of coupled two-dimensional partial (integro-) differential equations. This set can be approximated by a finite subset, which can be solved numerically. For this purpose we use the spline method [19].

The α particle will be labeled as particle one, the nucleons as particles two and three. We will ignore the isospin-symmetry breaking in most cases, and assume a pure $T = 0$ state for the ^{6}Li nucleus. We will perform one calculation which includes explicit isospin breaking, to check if this simplification is justified. The breaking is generated by including the Coulomb force, and considering the nucleons to have different masses. (We will consider particle two to be the neutron, and particle three to be the proton.)

For further discussion of the Faddeev equations in the notation above, and the numerical method used to solve them we refer to Ref. [19]. A more up-to-date description of our methods will be published at a later time. Now we will discuss the angular-momentum basis functions used in our calculations in some detail, since it is both enlightening and instructive.

The three Faddeev equations are numbered using the labels of the noninteracting, or *spectator* particles, i.e., Faddeev equation i has particle i as the spectator particle. The orbital momentum of the two interacting particles relative to each other in the Faddeev equation i is denoted by l_{x_i}, and the orbital momentum of the pair with respect to the spectator particle by l_{y_i}. (Note that for every Faddeev equation there is a natural Jacobi coordinate system. The corresponding Faddeev amplitude will be expressed in this particular coordinate system.)

For the pure isosinglet case two of the three Faddeev equations are dependent, so that we only have to solve two independent equations. Consider equation one, i.e., the equation in which the α particle is the spectator. Antisymmetry of the wave function demands that $l_{x_1} + s_{23} + t_{23}$ be odd (note that $t_{23} = T$), parity demands that $l_{x_1} + l_{y_1}$ be even. For the second Faddeev equation there is only the parity requirement. We will use jj' coupling, i.e., the coupling scheme $[(l_{x_i}s_{jk})j_{x_i}(l_{y_i}s_i)j_{y_i}]JM_J$. The Faddeev equations are solved including all channels which have $j_{x_i} \leq j_{\max}$, where $j_{\max}$ is varied to check the convergence. For the largest calculation we have used $j_{\max} = 8.5$, corresponding to 75 channels. For the case including isotriplet admixture we have to solve all three Faddeev equations. Also, the antisymmetry requirement is no longer present since we consider the two nucleons to be distinguishable, so that the number of channels doubles when compared to the corresponding isosinglet case.

Note that our calculations are complete in the sense that only states with very high two-body angular momenta are left out. This is a notable difference from most calculations in the literature which employ far fewer channels. The dependence of our results upon the number of channels and comparison with other calculations will be deferred until Sec. V.

To investigate the quality of the wave function, we study the longitudinal form factors and the associated moments as an example of the static properties of the wave function. The charge radius and quadrupole moment are given by

$$\langle r^2\rangle^{1/2} = (\tfrac{2}{3}\langle r_1^2\rangle + \tfrac{1}{3}\langle r_2^2\rangle)^{1/2}\,, \tag{5}$$

$$\langle Q\rangle = \sqrt{\tfrac{16\pi}{5}}[2\langle r_1^2 Y_{20}(\hat{\boldsymbol{r}}_1)\rangle + \langle r_2^2 Y_{20}(\hat{\boldsymbol{r}}_2)\rangle]\,. \tag{6}$$

They are related to the low-energy limit of the Coulomb form factors

$$\begin{aligned} F_{Cl}(q) &= \frac{\sqrt{4\pi}}{Z}\sum_i Z_i\langle J||Y_l(\hat{\boldsymbol{r}}_i)j_l(qr_i)||J\rangle \\ &= \frac{\sqrt{4\pi}}{Z}\sum_i \frac{Z_i}{\langle J\,J\,l\,0|J\,J\rangle}\langle J\,J|Y_{l0}(\hat{\boldsymbol{r}}_i)j_l(qr_i)|J\,J\rangle\,, \end{aligned} \tag{7}$$

where $Z = 3$ and $J = 1$ for ^{6}Li. The low-energy limit of F_{C0} (for point particles) is

$$\frac{\sqrt{4\pi}}{Z}\sum_i \frac{Z_i}{\langle 1\,1\,0\,0|1\,1\rangle}\langle 1\,1|Y_{00}(\hat{\boldsymbol{r}}_i)j_0(qr_i)|1\,1\rangle \longrightarrow \frac{1}{Z}\sum_i Z_i\langle 1\,1|1 - \tfrac{1}{6}(qr)^2|1\,1\rangle = 1 - \tfrac{1}{6}\langle r^2\rangle q^2\,. \tag{8}$$

The low-energy limit of F_{C2} is

$$\frac{\sqrt{4\pi}}{Z}\sum_i \frac{Z_i}{\langle 1\,1\,2\,0|1\,1\rangle}\langle 1\,1|Y_{20}(\hat{\boldsymbol{r}}_i)j_2(qr_i)|1\,1\rangle \longrightarrow \frac{\sqrt{4\pi}}{Z}\sum_i \frac{Z_i\sqrt{10}}{(2\times 2+1)!!}\langle 1\,1|Y_{20}(\hat{\boldsymbol{r}}_i)(qr)^2|1\,1\rangle = \frac{1}{3Z\sqrt{2}}Qq^2\,. \tag{9}$$

The inclusion of the Pauli principle will be discussed in Sec. IV. In the next section we will concentrate on the polarization of constituents.

III. POLARIZATION OF CONSTITUENTS

The question we want to ask is the following: if we pick a nucleon from the fully polarized nucleus ($J_Z = J$) without disturbing its spin, what are the odds for finding its spin "up." A similar description of polarization was first used in Ref. [11] for the case of ^{3}He.

We will follow a similar line of reasoning here; first for the case of the deuteron to establish notation and then for ^{6}Li. The quantity

$$P_n^+ = \langle J\,J|\hat{P}_n^+|J\,J\rangle, \tag{10}$$

where

$$\hat{P}_n^+ = \frac{1-\tau_3(1)}{2}\frac{1+\sigma_3(1)}{2} + \frac{1-\tau_3(2)}{2}\frac{1+\sigma_3(2)}{2} = P_n(1)P^+(1) + P_n(2)P^+(2) \quad (11)$$

and $|J\,J\rangle = |\Psi(J_Z = J)\rangle$ is the probability for the neutron to have its spin aligned "up." Due to the fact that the deuteron is in a pure $J = 1$, $T = 0$ state, as is ^{6}Li in models without isospin-symmetry breaking, the two nucleons have to be in the isosinglet state. This means that there is only one isospin function in the wave function, which can be factored out. This simplifies the calculations significantly, as we find

$$\begin{aligned} P_n^+ &= \langle T=0|P_n(1)|T=0\rangle\langle J\,J|P^+(1)|J\,J\rangle \\ &\quad + \langle T=0|P_n(2)|T=0\rangle\langle J\,J|P^+(2)|J\,J\rangle \\ &= \tfrac{1}{2}\langle J\,J|P^+(1)|J\,J\rangle + \tfrac{1}{2}\langle J\,J|P^+(2)|J\,J\rangle\,. \end{aligned} \quad (12)$$

The remaining matrix elements can be calculated by separating the spin and orbital parts using a simple case analysis. First we consider the deuteron which has the orbital momentum states $\{S, D\}$ coupled to the spin triplet state. Since spin projection operators leave orbital angular momenta invariant and there is exactly one spin state per orbital momentum state, there is no coupling between spin states, so that we find for the deuteron the diagonal terms:

$$\begin{aligned} \langle 11|P^+(i)|11\rangle &= P_S\langle(01)11|P^+(i)|(01)11\rangle \\ &\quad + P_D\langle(21)11|P^+(i)|(21)11\rangle\,, \end{aligned} \quad (13)$$

where P_S and P_D are the probabilities ($P_S + P_D = 1$) of the orbital angular momentum states $|(LS)JJ\rangle$ of the deuteron. The remaining matrix elements of (13) are of angular momentum functions only. They can be evaluated using

$$\langle(LS)JJ|P^+(i)|(LS)JJ\rangle = \sum_{MM'}\langle L\,M\,S\,M'|L\,S\,J\,J\rangle^2\langle S\,M'|P^+(i)|S\,M'\rangle\,.$$

Evaluating these matrix elements yields the simple and well-known result

$$P_n^+ = P_S + \tfrac{1}{4}P_D\,. \quad (14)$$

Now we turn to the polarization of the two "valence" nucleons of ^{6}Li since in our model the α particle is an elementary particle, and its constituents are therefore outside our grasp. If at first we neglect the isotriplet component of the wave function, the isospin function can be factored out and the possible orbital momentum states of the three-body system are $\{S, P, P', D\}$, where a prime is used in an unconventional way: to denote a state with odd l_{x_1}. The S, P, and D states are coupled to the spin triplet state, the P' is coupled to the spin singlet state. (Just as for the isospin sum, the absence of spin structure in the α particle simplifies matters enormously.) Again there is no coupling between spin states and we find

$$\begin{aligned} \langle 11|P^+(i)|11\rangle = \; & P_S\,\langle(01)11|P^+(i)|(01)11\rangle \\ & + P_P\,\langle(11)11|P^+(i)|(11)11\rangle \\ & + P_{P'}\langle(10)11|P^+(i)|(10)11\rangle \\ & + P_D\,\langle(21)11|P^+(i)|(21)11\rangle\,. \end{aligned} \quad (15)$$

The final result is very simple, and in contrast to the analog formula for ^{3}He, it is exact:

$$P_n^+ = P_S + \tfrac{3}{4}P_P + \tfrac{1}{2}P_{P'} + \tfrac{1}{4}P_D\,. \quad (16)$$

If, for some reason, only the total P state probability $P_{P_{\rm tot}}$ is known, we still have the following bound:

$$P_S + \tfrac{1}{2}P_{P_{\rm tot}} + \tfrac{1}{4}P_D \le P_n^+ \le P_S + \tfrac{3}{4}P_{P_{\rm tot}} + \tfrac{1}{4}P_D\,. \quad (17)$$

We remark that from the corresponding analysis for the proton it follows that $P_n^+ = P_p^+$ in this model of $T = 0$ ^{6}Li (and in the deuteron).

The Coulomb interaction does not conserve isospin so that a ^{6}Li model with the Coulomb force is not a pure $T = 0$ state but has a small admixture of $T = 1$. Because there is more than one isospin state there can be more than one spin state per angular momentum state. This means that the diagonal probabilities cannot be used in all cases. The analysis outlined above is unchanged for the S and D states, however, because the spin triplet state cannot couple to the spin singlet (since there is no spin singlet component in these states). Hence the S- and D-state contributions to P_n^+ can still be written in terms of probabilities. For the P and P' states the $T = 1$ admixture allows more than one spin state per orbital momentum state and the best one can do is derive the following bound in terms of the total P-state probability:

$$P_S + \tfrac{1}{4}P_{P_{\rm tot}} + \tfrac{1}{4}P_D \le P_n^+ \le P_S + P_{P_{\rm tot}} + \tfrac{1}{4}P_D\,. \quad (18)$$

We note that this bound is not as tight as the (unnecessary) bound derived above for the isospin-symmetric model. Finally, although the *bounds* are the same for the polarization of the neutron and the proton,

$$P_n^+ \neq P_p^+ \quad (19)$$

in this most realistic three-body model of ^{6}Li. In practice, the difference is small because $P_{P_{\rm tot}} \approx 3\%$.

It is important to emphasize that the formulas derived above for the polarization of the constituents of ^{6}Li are intended to develop an intuition for our numerical results. The values of P_n^+ presented in the tables for the various Hamiltonians did not come from these formulas but were calculated exactly in the codes.

IV. αN AND NN POTENTIALS

We will neglect the microscopic structure of the α particle. Its structure is partially represented by the αN interaction and by its charge form factor. The αN potentials we will use are of a phenomenological nature: they more or less fit the αN low-energy phase shifts. However, most potentials support a deeply bound αN state, which contradicts experimental observation. The justification

for this seeming discrepancy is thought to be the Pauli principle which excludes this bound state.

The Pauli principle can be taken into account in several essentially different ways. First, one can use a potential that is repulsive in the s state, so that no forbidden bound state is supported. Second, one can suppress the forbidden bound state, by replacing the Hamiltonian H by

$$H' = PHP\,, \tag{20}$$

where P is an operator that projects out the forbidden states:

$$P = (1 - |\psi_2\rangle\langle\psi_2|)(1 - |\psi_3\rangle\langle\psi_3|)\,, \tag{21}$$

where $|\psi_i\rangle$ is the forbidden two-body bound state of particles j and k. Another possibility is to suppress not the Pauli-forbidden state itself, but some harmonic-oscillator state close to it.

The relative merits of the two different methods have been studied phenomenologically for some time now. The experimental properties of the three-body system appear not to distinguish between these choices [20,21]. Supersymmetric quantum mechanics provides a new tool for studying the application of the Pauli principle to scattering of a projectile from a composite system. That is, it is always possible to generate from a given local deep (shallow) potential a corresponding shallow (deep) potential which produces the same phase shifts [22]. The scalar Hamiltonians H_0 and H_2 associated with these "phase equivalent" potentials can be represented as components of a supersymmetric Hamiltonian which act in subspaces of an overall supersymmetric space [23]. These subspaces are analogous to the bosonic and fermionic sectors in supersymmetric formulations of field theory [24]. Given H_0 (H_2) we can derive H_2 (H_0) by means of a supersymmetric transformation. This has been done for an $\alpha\alpha$ interaction [22] and for the αN interaction [25]. The phase equivalent shallow potential has a repulsive r^{-2} singularity for small r in agreement with the notion that Pauli effects for composite systems are repulsive in the range of wave-function overlap. Although the supersymmetric transformation provides a unique local potential that gives the scattering and has no Pauli-forbidden bound state, to our knowledge, there are no few-body calculations which probe the off-shell properties of the supersymmetric partners. This subject and the different methods for handling the problem of unphysical s-wave bound states generated by αN potentials will be discussed in detail in a subsequent publication.

The method we have used in our calculations is a variation of the second approach. We replace the αN potentials V_i by

$$V_i' = V_i + \Gamma|\psi_i\rangle\langle\psi_i|\,, \tag{22}$$

and let the (positive) constant Γ go to infinity. We will show that this limit can be taken analytically, and that in the limit this method is exactly equivalent to solving the three-body equation in the restricted space.

The resolvent for the two-body Schrödinger operator

$$H' = H_0 + V + \Gamma|\psi_f\rangle\langle\psi_f| \tag{23}$$

can be written as

$$G'(E) = G(E) - \frac{|\psi_f\rangle\langle\psi_f|}{(E - E_f)(1 - \frac{E-E_f}{\Gamma})}\,,$$

where $G(E)$ is the resolvent when $\Gamma = 0$, $|\psi_f\rangle$ a Pauli-forbidden state, and E_f its bound-state energy. Using this expression in Faddeev equation i by embedding it in three-body space, we find

$$|\psi_i\rangle = \left(G_i - \int \mathrm{d}^3\boldsymbol{q}_i \frac{|\boldsymbol{q}_i\psi_{if}\rangle\langle\boldsymbol{q}_i\psi_{if}|}{(E - E_{if} - q_i^2)(1 - \frac{E-E_{if}-q_i^2}{\Gamma})}\right) V_i'(|\psi_j\rangle + |\psi_k\rangle)\,, \tag{24}$$

where $\boldsymbol{q}$ is the spectator momentum. When Γ is large, we can approximate this by

$$\begin{aligned}|\psi_i\rangle &= \left(G_i - \int \mathrm{d}^3\boldsymbol{q}_i \frac{|\boldsymbol{q}_i\psi_{if}\rangle\langle\boldsymbol{q}_i\psi_{if}|}{E - E_{if} - q_i^2}[1 + \Gamma^{-1}(E - E_{if} - q_i^2) + O(\Gamma^{-2})]\right)\left(V_i + \Gamma\int \mathrm{d}^3\boldsymbol{q}_i'|\boldsymbol{q}_i'\psi_{if}\rangle\langle\boldsymbol{q}_i'\psi_{if}|\right)(|\psi_j\rangle + |\psi_k\rangle)\\ &= G_i(V_i + \Gamma P_{if})(|\psi_j\rangle + |\psi_k\rangle) - \int \mathrm{d}^3\boldsymbol{q}_i \frac{|\boldsymbol{q}_i\psi_{if}\rangle\langle\boldsymbol{q}_i\psi_{if}|}{E - E_{if} - q_i^2}(V_i + \Gamma)(|\psi_j\rangle + |\psi_k\rangle)\\ &\quad -P_{if}(\Gamma^{-1}V_i + 1)(|\psi_j\rangle + |\psi_k\rangle) + O(\Gamma^{-1})\,,\end{aligned} \tag{25}$$

where we have written P_{if} to denote

$$\int \mathrm{d}^3\boldsymbol{q}_i|\boldsymbol{q}_i\psi_{if}\rangle\langle\boldsymbol{q}_i\psi_{if}|\,. \tag{26}$$

(Note that $P_{if}^2 = P_{if}$ and that $[P_{if}, G_i] = [P_{if}, H_i] = 0$.) Using the fact that

$$G_iP_{if} = \int \mathrm{d}^3\boldsymbol{q}_i \frac{|\boldsymbol{q}_i\psi_{if}\rangle\langle\boldsymbol{q}_i\psi_{if}|}{E - E_{if} - q_i^2}\,, \tag{27}$$

we finally arrive at

$$\begin{aligned}|\psi_i\rangle = G_i(1 - P_{if})V_i(|\psi_j\rangle + |\psi_k\rangle) - P_{if}(|\psi_j\rangle + |\psi_k\rangle)\\ +O(\Gamma^{-1})\,.\end{aligned} \tag{28}$$

To prove that this equation gives the correct solution in the limit $\Gamma \to \infty$, we must show that (in this limit)

$$(1 - P_{if})(E - H)|\Psi\rangle = P_{if}|\Psi\rangle = 0\,. \tag{29}$$

Multiplying Eq. (28) by P_{if}, we find

$$P_{if}(|\psi_i\rangle + |\psi_j\rangle + |\psi_k\rangle) = P_{if}|\Psi\rangle = 0\,. \tag{30}$$

This proves the first condition, provided that Eq. (3) defines the correct Schrödinger wave function. Now we multiply Eq. (28) with $(E - H_i)$:

$$\begin{aligned}(E - H_i)|\psi_i\rangle &= (1 - P_{if})V_i(|\psi_j\rangle + |\psi_k\rangle) \\ &\quad -(E - H_i)P_{if}(|\psi_j\rangle + |\psi_k\rangle) \\ &= V_i(|\psi_j\rangle + |\psi_k\rangle) \\ &\quad -P_{if}(E - H_0)(|\psi_j\rangle + |\psi_k\rangle)\,. \end{aligned} \tag{31}$$

Now use Eq. (4) to eliminate $|\psi_j\rangle$ and $|\psi_k\rangle$ from the right-hand side:

$$(E - H_i)|\psi_i\rangle = V_i(|\psi_j\rangle + |\psi_k\rangle) - P_{if}(V_j + V_k)|\Psi\rangle\,, \tag{32}$$

which, when added to the two remaining Faddeev equations gives

$$(E - H_0)|\Psi\rangle = -P_{if}(V_j + V_k)|\Psi\rangle\,. \tag{33}$$

We now multiply with $(1 - P_{if})$ to complete our proof:

$$\begin{aligned}&(1 - P_{if})(E - H_0)|\Psi\rangle \\ &\qquad = (1 - P_{if})(E - H_0)(1 - P_{if})|\Psi\rangle = 0\,, \end{aligned} \tag{34}$$

showing that the second condition we needed is satisfied, and that $|\Psi\rangle$ is indeed a solution of the Schrödinger equation in the restricted space, as we claimed earlier.

We will now discuss the potentials actually used by us in this paper. The nucleon-nucleon potentials used are the Reid soft core potential (RSC) [26], the super soft core potential (SSC) [27], and the (s-wave) Malfliet-Tjon I-III potential (MT) [28]. The RSC and SSC potentials are realistic nucleon-nucleon interactions, and have a tensor force. The MT potential is a simple model without a tensor force, but it is very popular in the literature. The alpha-nucleon potentials used are the simple Sack-Biedenharn-Breit potential (SBB) [29] of which we use three versions, a potential with the Wood-Saxon form of Satchler *et al.* (SAT) [30], and one of the potentials obtained on a grid from an inversion of proton-alpha scattering data by Cooper and Mackintosh (CM) [31].

There is considerable confusion over the parameters of simple model potentials. The exact parameters of the potentials we use are given in Table I. The algebraic forms are

$$V_{\rm MT} = V_1\frac{e^{-\mu_1 r}}{r} + V_2\frac{e^{-\mu_2 r}}{r}\,,$$

for the Malfliet-Tjon NN potential [28],

$$V_{\rm SBB} = V_1 e^{-(r/\mu_1)^2} + (\boldsymbol{l}\cdot\boldsymbol{s})V_2 e^{-(r/\mu_2)^2}\,,$$

for the Sack-Biedenharn-Breit αN potential [29], and

$$V_{\rm SAT} = V_c + (\boldsymbol{l}\cdot\boldsymbol{s})\frac{1}{r}\frac{d}{dr}V_{ls}\,,$$

where

$$V_{c,ls} = \frac{V_1}{1 + e^{(r-\mu_1)/\mu_2}}\,,$$

TABLE I. Parameters of the nucleon-nucleon and alpha-nucleon potentials used. Parameters are in appropriate powers of MeV and fm.

Potential	Component	V_1	μ_1	V_2	μ_2
MT	Singlet	−513.968	1.550	1438.720	3.110
	Triplet	−626.885	1.550	1438.720	3.110
SBB		−47.32	2.30	5.8555	2.30
SBB_2	S, P	−47.32	2.30	5.8555	2.30
	D	−23.00	2.30		
SBB_3	S	+50.00	2.30		
	P	−47.32	2.30	5.8555	2.30
	D	−23.00	2.30		
SAT	Central	−43.0	2.00		0.70
	$\boldsymbol{l}\cdot\boldsymbol{s}$	+40.0	1.50		0.35

for the Satchler αN potential. The optical model potential of Satchler *et al.* [30] has traditionally been modified for three-body calculations by neglecting the energy dependence of μ_1 [32,33] and refitting the parameters. We make the same approximation and use the parameters of Refs. [32,33].

Both potentials SBB and SAT have the same radial form for odd- and even-parity potentials, in contrast to effective local potentials which are deemed equivalent to the nonlocal interaction obtained from resonating-group model (RGM) calculations (see, for example, Fig. 26 of [34]). The source of the parity dependence in RGM calculations is exchange processes. To examine this odd-even feature of αN potentials, we also use the CM potential which is strongly parity dependent; having short-range even-parity potentials and long-range odd-parity potentials. The energy dependence of the CM potential, obtained by an inversion procedure, is rather less than that of SAT which arises from a direct optical model fit of the data. We make the usual energy-independent approximation (which should be better for the CM potential) by choosing the 12 MeV version as shown in Fig. 4 of Ref. [31].

The RSC and SSC potentials are as defined in [26,27], respectively. We used the exact physical masses for all constituents. For systems without isospin breaking, we used the average mass of the proton and the neutron as the nucleon mass. We used two different Coulomb potentials. The first, taken from [35], is

$$V = \begin{cases} \dfrac{2e^2}{2R}(3 - (r/R)^2), & r < R, \\ \dfrac{2e^2}{r}, & r \geq R, \end{cases}$$

where $R = 1.25 \times 4^{1/3}$ fm. The second, taken from [32], is

$$V = \frac{2e^2}{r}\,\mathrm{erf}(r/a)\,,$$

where $a = \sqrt{\frac{2}{3}} \times 1.64$ fm.

V. SOURCES OF UNCERTAINTY

In this section we will discuss the results obtained with our method for various models and the various sources of uncertainty. These can be separated into numerical uncertainties, which will be discussed first, and the uncertainties due to uncertainties of the input: the interactions between the constituents. The validity of the three-body model will be not be discussed here, but we will comment on it in the next section.

A. Numerical approximations

There are three types of numerical approximations in our calculations, one of which can (and will be) avoided, and two which are unavoidable. The approximations are (i) the forbidden state is not projected out but suppressed using a separable term as in Eq. (22); (ii) the spline approximation, the accuracy of which is determined by the number of intervals in which the domain of the partial differential equation is subdivided; and (iii) the partial-wave series is approximated by a finite number of partial waves. (Note that for potentials defined on a finite number of partial waves, the results are exact if all these partial waves are included in the calculation.) The errors associated with approximations (i) and (ii) reduce systematically as the suppression parameter Γ and the number of intervals in the grid are increased. This is illustrated by Tables II and III. The error associated with approximation (iii) is not as easily expressed as a function of the relevant parameter ($j_{\max}$), so that only very crude extrapolations can be made, and it is essential to use a very high number of channels. This is shown in Table IV. It appears that $j_{\max} = 6.5$ is sufficient to calculate all the observables with a precision that is better than or comparable to that of experiment.

For most models, it is possible to make Γ extremely large $O(10^8)$, so that we actually reach "infinity" for all practical purposes. Another possibility is to take the limit analytically in the manner we have shown earlier. This was done for almost all calculations. Table II shows that all the observables converge nicely to the value for $\Gamma = \infty$, and do so with leading Γ^{-1} behavior, as expected. (Note that Γ is expressed in units of $\hbar^2/M$, where M is approximately one nucleon mass. The exact value of $\hbar^2/M$ is 41.47 MeV fm^2.)

As is well known [19], the error of a spline approximant is $O(h^4)$ (where h is the length of an interval in the grid), provided h is sufficiently small. This fact can be exploited, by taking suitable linear combinations of results obtained for different grid sizes, which effectively means extrapolating to an infinitely fine grid. The observed deviations from fourth-order convergence are used to estimate the error.

We would like at this moment to stress a very interesting point, which is often neglected and has led to confusion. It is illustrated by Table IV: the Faddeev eigenvalue E_F and the expectation value of the Hamiltonian $\langle H \rangle$ differ substantially. This difference decreases when the number of channels increases. The explanation for this phenomenon is the following: Solving the Faddeev equations for a certain set of partial waves is exactly equivalent to solving the Faddeev equations for all partial waves if the two-body potentials V_i are restricted to operate in these partial waves only. Therefore, if we evaluate $\langle H^* \rangle$ where H^* is the Hamiltonian in which the potentials are restricted to operate in the set of partial waves for which we solved the Faddeev equations, we will find it to be equal to E_F.

However, the expectation value of the full Hamiltonian H will be different from $\langle H^* \rangle$. This can be understood as follows: the total (Schrödinger) wave function is the sum of the three Faddeev amplitudes. These three amplitudes can be written using a finite number of channels, provided the expansion is done in the natural (Jacobi-) coordinate system of each amplitude. After adding the amplitudes this is no longer possible, since a state that has good quantum numbers l_x and l_y in one coordinate system does in general not have corresponding good quantum numbers in any other system. The total wave function therefore contains an infinite number of angular-momentum components. The full Hamiltonian operates in all channels, so that there will be a contribution to $\langle H \rangle$ from these *induced* channels.

Usually, the potentials are attractive. This means that $\langle H \rangle$ will be below $\langle H^* \rangle$. In other words: it will be closer to the exact (ground-state) energy. This is why a wave function constructed from Faddeev amplitudes with a certain number of channels is usually closer to the full wave function than a wave function obtained from a direct solution of the Schrödinger equation for the same number of channels.

Extrapolation to an infinite number of channels is very

TABLE II. Influence of forbidden-state admixture for model a, 10×10 grid, $j_{\max} = 2.5$. The number in parentheses is the estimated uncertainty in the last digit.

Γ ($\hbar^2$/M)	E_F (MeV)	$\langle H \rangle$ (MeV)	P_F	$\langle r^2 \rangle^{1/2}$ (fm)	Q (e fm^2)	P_n^+ (%)
10^0	−3.998062	−4.8716(4)	5.3750×10^{-3}	2.512(1)	0.5541(2)	93.1589(1)
10^1	−3.780032	−4.4108(4)	8.3528×10^{-5}	2.565(1)	0.5612(3)	93.3229(1)
10^2	−3.745151	−4.3373(4)	1.0866×10^{-6}	2.576(1)	0.5622(3)	93.3309(1)
10^3	−3.740991	−4.3281(4)	1.0637×10^{-8}	2.577(1)	0.5623(3)	93.3316(1)
10^4	−3.740564	−4.3272(4)	4.9040×10^{-10}	2.577(1)	0.5623(3)	93.3316(1)
10^5	−3.740521	−4.3271(4)	4.9909×10^{-10}	2.577(1)	0.5623(3)	93.3316(1)
10^6	−3.740517	−4.3270(4)	5.1056×10^{-10}	2.577(1)	0.5623(3)	93.3316(1)
10^7	−3.740516	−4.3270(4)	5.1137×10^{-10}	2.577(1)	0.5623(3)	93.3316(1)
∞	−3.740516	−4.3270(4)	5.1153×10^{-10}	2.577(1)	0.5623(3)	93.3316(1)

TABLE III. Convergence of the spline approximation for model a, $j_{max} = 2.5$.

Grid	E_F (MeV)	$\langle H \rangle$ (MeV)	E_{Coul} (MeV)	$\langle r^2 \rangle^{1/2}$ (fm)	Q (e fm^2)	P_n^+ (%)
10×10	−3.7405(1)	−4.3270(4)	0.8998(2)	2.577(1)	0.5623(3)	93.3316(1)
14×14	−3.7840(1)	−4.3375(2)	0.9006(2)	2.570(1)	0.5482(3)	93.3297(2)
20×20	−3.7889(1)	−4.3427(2)	0.9011(2)	2.570(1)	0.55171(7)	93.3267(1)
28×28	−3.7910(1)	−4.3433(2)	0.9013(2)	2.570(1)	0.55299(5)	93.3257(1)
$\infty \times \infty$	−3.7917(4)	−4.3434(2)	0.9014(2)	2.570(1)	0.5534(2)	93.3254(1)

difficult, and we have used it very conservatively. We are confident that the errors listed (the number in parentheses is the uncertainty in the last quoted digit) are not too small. (A confirmation of this can be found in Table IV, by comparing the extrapolated values of E_F and $\langle H \rangle$: the difference between the two is well within the error bars.) The rest of the results presented in this paper are the result of extrapolation to infinite grid size and an infinite number of channels, i.e., they are absolute predictions of ^{6}Li observables in the three-body model.

B. Models

We have performed full calculations for eight different interaction models. The models used are (a) RSC+SBB, (b) RSC+SBB with isospin breaking, (c) RSC+SBB$_2$, (d) RSC+SBB$_3$, (e) RSC+SAT, (f) RSC+CM, (g) SSC+SBB, and (h) MT+SBB. Note that only model b has isospin breaking. We will also display partial results for some of these models where the strong interaction is augmented by the Perey-Perey Coulomb force (but ignoring its isospin breaking). These results are labeled (a*) RSC+SBB, (e*) RSC+SAT, (f*) RSC+CM, (g*) SSC+SBB, and (h*) MT+SBB.

Models a, a*, and b are used as reference models, since they describe the lithium observables very well (provided the Coulomb force is included, either directly as in a* and b, or by perturbation theory). Note that we assume the SBB potential to interact in all partial waves, since we feel that a realistic interaction cannot have interaction in the lowest partial waves only. Model c contains the SBB potential in a somewhat modified form (SBB$_2$), as suggested by Bang *et al.* [36]. The modifications are twofold: (i) the d-wave interaction is attenuated to better fit the phase shifts, (ii) the potential only works in s, p, and d waves. Model d contains a third version of the SBB potential [37], which replaces the attractive Gaussian s-wave potential of SBB$_2$ by a repulsive one and therefore does not support a forbidden state. In this SBB$_3$ the p-wave and $\boldsymbol{l} \cdot \boldsymbol{s}$ parameters are those of the original SBB, the d-wave strength is attenuated, and, of course, the s-wave potential is repulsive. Models e and f retain the RSC potential as the NN interaction but enlarge the range of alpha-nucleon interactions studied. Finally models g and h return to the SBB alpha-nucleon potential but vary instead the nucleon-nucleon interaction. Parameters of the potentials we use are given in Table I and in Refs. [26,27] for the RSC and SSC nucleon-nucleon potentials. Note that the values in Table I may differ slightly from the original references.

C. Model dependence

We will now discuss the effect of variations of different parameters in our model. These are (i) the manner in which the Pauli principle is taken into account in the alpha-nucleon interaction, (ii) the presence or absence of isospin-symmetry breaking, (iii) different forms of the αN interactions, and (iv) different forms of the NN interactions.

Looking at Table V and comparing models c and d we see that there is little difference between the two models. In the case of ^{6}Li it hardly matters whether potentials supporting Pauli-forbidden states in the s wave (e.g., c) or repulsive potentials (e.g., d) are used. The only difference seems to be that the attractive potential binds ^{6}Li marginally less strong. This appears to be a confirmation of the results of Lehman [20,21] obtained with separable αN potentials.

Comparing models a, a*, and b we see that although there is (probably because ^{6}Li is so lightly bound) substantial isospin-symmetry breaking (the effect on the binding energy is about 0.15 MeV), it appears that only the binding energy and the charge radius are substantially affected. The other observables are hardly changed at all. It therefore seems justified to ignore the $T = 1$ components, provided that one bears in mind that a noticeable energy effect is to be expected.

The influence of the form of the αN interaction is rather large, as Table V shows. This is to be expected

TABLE IV. Convergence of the partial-wave series for model a, 20×20 grid.

j_{max}	E_F (MeV)	$\langle H \rangle$ (MeV)	E_{Coul} (MeV)	$\langle r^2 \rangle^{1/2}$ (fm)	Q (e fm^2)	P_n^+ (%)
KUK	−3.4983(1)	−4.1098(2)	0.8688(2)	2.663(1)	0.2232(1)	94.2981(1)
2.5	−3.7889(1)	−4.3427(2)	0.9011(2)	2.570(1)	0.55171(7)	93.3267(1)
4.5	−4.2079(1)	−4.4336(2)	0.9304(2)	2.4848(8)	0.59616(5)	92.8454(1)
6.5	−4.3655(1)	−4.4481(2)	0.9390(2)	2.4595(6)	0.58570(4)	92.7861(1)
8.5	−4.4212(1)	−4.4509(2)	0.9411(2)	2.4523(6)	0.57658(4)	92.7876(1)
∞	−4.45(2)	−4.4518(6)	0.9418(5)	2.450(2)	0.573(5)	92.788(1)

TABLE V. Overview of results for 13 different systems.

Model	$\langle H \rangle$ (MeV)	E_{Coul} (MeV)	$\langle r^2 \rangle^{1/2}$ (fm)	$P_{\alpha \mathrm{D}}$ (%)	Q (e fm^2)	P_n^+ (%)
a	−4.452(1)	0.942(1)	2.450(2)	67.47(2)	0.573(5)	92.788(1)
b	−3.365(6)	0.932(2)	2.617(4)	68.89(4)	0.585(5)	92.796(3)
c	−3.629(1)	0.892(1)	2.616(1)	70.15(1)	0.520(1)	93.626(1)
d	−3.662(1)	0.869(1)	2.625(1)	71.12(1)	0.547(1)	93.310(1)
e	−4.081(1)	0.923(1)	2.509(6)	67.34(4)	0.605(4)	92.254(2)
f	−3.344(1)	0.927(1)	2.564(9)	71.17(3)	0.420(2)	94.111(3)
g	−4.281(1)	0.934(1)	2.474(4)	66.88(3)	0.582(3)	93.730(1)
h	−4.389(1)	0.952(1)	2.444(2)	62.42(2)	0.256(1)	98.123(2)
a*	−3.516(2)	0.910(1)	2.542(4)	69.05(4)	0.578(5)	92.953(2)
e*	−3.162(1)	0.883(1)	2.646(3)	69.46(5)	0.598(4)	92.559(2)
f*	−2.444(1)	0.841(2)	3.040(8)	75.64(8)	0.405(8)	94.275(4)
g*	−3.352(1)	0.900(1)	2.585(2)	68.62(3)	0.589(3)	93.896(1)
h*	−3.440(1)	0.919(1)	2.544(2)	63.98(2)	0.258(1)	98.277(1)

since there is not nearly as much consensus on this interaction as there is on the NN interaction. This is due to the composite structure of the alpha particle, the amount of experimental data available, and finally the number and quality of αN model interactions available. The use of high-precision inversion techniques is a rather recent development. The structure of the alpha particle and the amount of data available make the inversion rather difficult, since there is a large amount of nonlocality (which can be expressed as energy dependence or dependence on the angular momentum) and uncertainty in the interaction.

It is somewhat disappointing to see that the rather crude potentials SBB and SAT reproduce the ^{6}Li binding energy much better than the more sophisticated CM potential, especially since this potential yields an attractively low value for the quadrupole moment Q (we will discuss the sign of the quadrupole moment later on). It is known that the ground-state energy of ^{6}Li in a three-body model is not sensitive to phase shifts at higher energy of the αN interaction and that low-energy phase shift properties of the potential are the most important for this purpose [38]. We checked the s-wave phase shifts of the three potentials and found that the SBB and SAT reproduced the threshold behavior [39] much better than did the CM potential. It is possible that a slight refit of the CM potential which emphasizes threshold behavior could yield a much better ^{6}Li model.

We found the two αp Coulomb models to be hardly distinguishable: the Coulomb energy for the Perey-Perey model was systematically about 8 keV larger than that for the error-function model. This is a negligible difference when compared to the uncertainties encountered earlier.

Often, the Coulomb potential is treated as a perturbation. Looking at Table V, we see that the difference of the ground-state energy plus Coulomb energy of a system and the ground-state energy of this system in which the Coulomb potential is taken into account exactly is about 5 keV (except for the very lightly bound system f, there the difference is about 27 keV), indicating that first-order perturbation theory for the Coulomb potential is a very good approximation of the $T = 0$ approximation of ^{6}Li (even though the Coulomb energy is relatively large, when compared to other nuclear systems), and therefore a fairly good approximation of the full system, yielding errors of a few percent (caused mainly by symmetry breaking, which is a higher-order effect).

Comparing models a, g, and h, which share the SBB αN interaction and vary the NN interaction, we see that the influence of the NN interaction on most observables is very small. However, model h has a substantially lower value for Q. This is due to the absence of a tensor force in this model (which implies much lower P- and D-state probabilities). Note also, that as a consequence of this, the predicted polarization of the valence nucleons is significantly larger than for the other models.

D. Summary

Summarizing, we think that within the three-body model (i) the numerical uncertainties in this work are negligible, (ii) ignoring the Coulomb potential in the Hamiltonian does not invalidate the general predictions that can be made, and (iii) by far the greatest source of uncertainty is the αN potential. (However, general properties are described rather well, provided the potentials fit the low-energy scattering data.)

VI. QUALITY OF THE THREE-BODY MODEL

Having established the main source and the magnitude of uncertainty within our model, we continue with a discussion on the quality of the three-body model itself by comparing with experiment and with other calculations found in the literature.

A. Comparison with experiment

In Fig. 1 we have plotted the charge radius as a function of the binding energy, and find that the points scat-

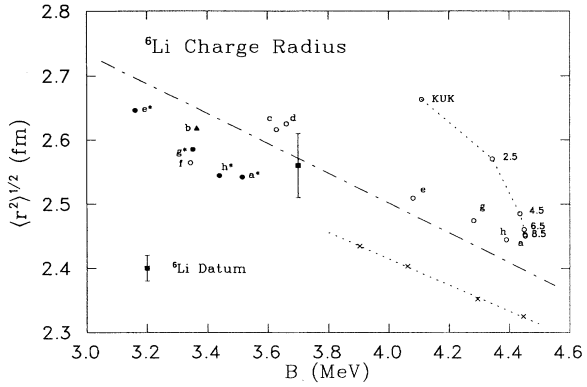

FIG. 1. The charge radius of ^{6}Li vs the binding energy B for breakup into α+n+p. The converged results of the models with different local potentials are labeled as in the text. Open circles are models without the Coulomb interaction and the solid symbols include the Coulomb interaction. The solid circles labeled "a*" include Coulomb but assume a pure $T = 0$ state. Our one complete calculation which included isospin breaking of the Coulomb force is the solid triangle. Also shown is the convergence of results of a single model (model a) with the number of channels. The straight line through our points is to guide the eye; it is the result of a least squares fit to all the local potentials considered. The results plotted as $\times$'s are from Ref. [43] which displays converged results from separable potentials fitted to the same parametrization of αN phase shifts. For this reason, they cluster more tightly around their least squares fit.

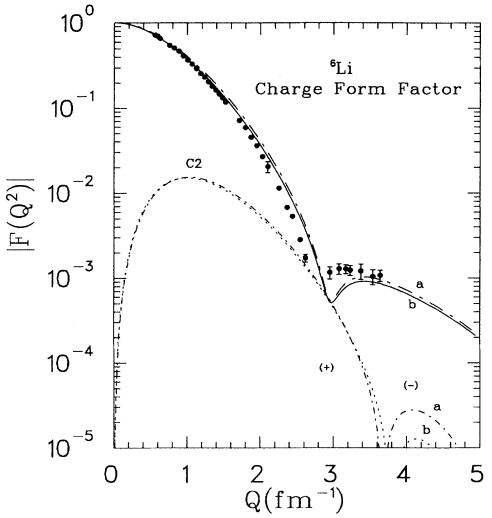

FIG. 2. The charge form factors of ^{6}Li vs momentum transfer. Model a does not have the Coulomb force and model b contains the Coulomb force including isospin breaking. The contribution of the quadrupole form factor $C2$ is also shown for these two models.

ter around a line, which goes through the experimental datum. We find this very encouraging, since it appears that three-body models can accurately describe the general features of the ^{6}Li nucleus. As Fig. 1 shows, it is only possible to draw such a conclusion about a fit to the experimental datum if a sufficiently large number of channels is used. If the number of channels is too small, the charge radius will be automatically too large. This effect can be substantial even when the energy appears to have converged, since an error of magnitude ε in the wave function will result in an error of $O(\varepsilon^2)$ in the binding energy and an error of $O(\varepsilon)$ in the other observables. This is more or less in agreement with the suggestion by Bang and Gignoux [33] who claim their binding energy has converged although they use a small number of channels. We remind the reader that the results presented in Fig. 1 and the latter tables are the result of extrapolation to infinite grid size and an infinite number of channels, i.e., they are absolute predictions of ^{6}Li observables in the three-body model.

Comparing the results in Table V for models a and b, we find that the Coulomb force does not play a very important role in ^{6}Li, apart from lowering the binding energy by approximately 0.9 MeV, and increasing the charge radius accordingly. In Fig. 2 we show the longitudinal form factors up to a four-momentum transfer of 5 fm^{-1} for models a and b. We used the impulse approximation of Eqs. (7)–(9) modified by folding in the nucleon [40] and alpha-particle [41] electromagnetic form factors. Our calculation predicts the experimental data [42] rather well up to about $q = 2.5$ fm^{-1}. The good agreement with experiment reflects the accuracy of our charge radius for these models and the fact that the dominant monopole term swamps the effect of the quadrupole term in this region. However, since the zero in the $C2$ contribution [i.e., F_{C2}, cf. Eq. (7)] occurs at somewhat higher q than that of the $C0$, we expect the agreement to be less good in the region of the diffraction minimum at about 3.0 fm^{-1}.

Our quadrupole form factor is close to that obtained by Eskandrian *et al.* [43], and rather different from that obtained by Kukulin *et al.* [44]. We find that the form factors for models a and b are very close to each other, again confirming that the Coulomb potential is not very important to the charge form factor. Our result does not support the suggestion by Kukulin *et al.* [44] that the disregard of the Coulomb force by Bang and Gignoux and by Lehman and co-workers is the cause of their overestimate of the theoretical $C0$ form factor in the region up to the first minimum. A recent preprint from Kukulin *et al.* [45] demonstrates that much of the disagreement of [44] with Bang and Gignoux, with Lehman and co-workers, and with us, on $C0$ and $C2$ (and many other predictions of their wave function) was caused by a severe truncation in partial waves of their variational wave function. Their truncation difficulties will be discussed further on in this section, but here we note that the new [45] $C2$ form factor from that group is consistent with Fig. 2.

Figure 2 shows the absolute prediction of the longitudinal form factor of ^{6}Li for our interaction models a and b which are described by a neutron, a proton, an α particle, and their interaction operators. We have not attempted to calculate meson-exchange contributions (MEC's) to this "impulse approximation" in order to be consistent with our other predictions of observables and with our

predictions of constituent polarizations. These latter predictions also drop corrections of relativistic order. This is because there are interaction-dependent ambiguities which arise from separating a completely relativistic result (which we do not have) into a nonrelativistic part plus corrections. For us the most analogous nucleus to ^{6}Li is the isoscalar-vector deuteron where these ambiguities in calculating the MEC to the $q \to 0$ charge radius and quadrupole moment are not large [46] and the corrections themselves are small. At higher momentum transfer, the MEC become larger and the interaction-dependent ambiguities also become of greater concern. One particular prescription which ties much but not all of the MEC to the interaction operator indicates that the pion seagull contribution is largest and of opposite sign to the dominant impulse approximation for F_L of the deuteron [47]. That is, the diffraction minimum is shifted to slightly lower q and the second maximum is enhanced by MEC. If one could confidently apply these (model-dependent) deuteron results to the case of ^{6}Li, one would conclude that our result of an impulse approximation form factor slightly above the data for higher q is further confirmation of the essential correctness of our models a and b. For this paper, we simply state that our calculated F_L is a direct prediction of the interaction model and that it agrees with the data at low momentum transfer.

To conclude the discussion of Table V, we briefly look at the α-D clustering probability, and the Coulomb energy. Although these are not observables, they do provide a crude consistency test: one expects scaling between the charge radius and the Coulomb energy and (since the binding energy as well as the clustering probability mainly depend on the strength of the αD interaction) scaling between the binding energy and the clustering probability. Table V confirms these expectations. The results are also in reasonable agreement with those found in the literature.

We will now turn to the magnetic moment, which is the $q \to 0$ limit of the transversal form factor. We will use the observation of Lehman *et al.* [48] and others that the magnetic moment for the ground state of ^{6}Li can be written in terms of probabilities:

$$\mu = \mu_p + \mu_n + (\tfrac{1}{2} - \mu_p - \mu_n)[\tfrac{1}{2}P_P + P_{P'} + \tfrac{3}{2}P_D]\,. \quad (35)$$

This simple formula has been criticized by Danilin *et al.* [37] as arising from a shell model which does not make allowance for the motion of the α particle, but they also show that the α orbital motion gives a contribution of 0.1% to the magnetic moment. Meson-exchange current contributions to the magnetic moment are isoscalar and therefore of order v^2/c^2 [49]. Such relativistic corrections should be consistently neglected in calculations such as ours. In any event, we calculate the magnetic moments of our models with (35) and display the results in Table VII and Fig. 3. The straight-line relationship between μ and P_n^+ is inherent in the formulas and introduces no new results. However, it is a test of self-consistency. (Note that model b is slightly off the dashed line. This is caused by the fact that the neutron polarization in model b cannot be expressed as wave-function probabilities, due to isospin breaking. If we were to plot the average polarization of the neutron and the proton for this model, it would again be exactly on the line.) It is gratifying to see that models a and b which have binding energies, longitudinal form factors, and charge radii in excellent agreement with experiment also predict a magnetic moment within 1% of the experimental value of 0.822 05 nuclear magnetons.

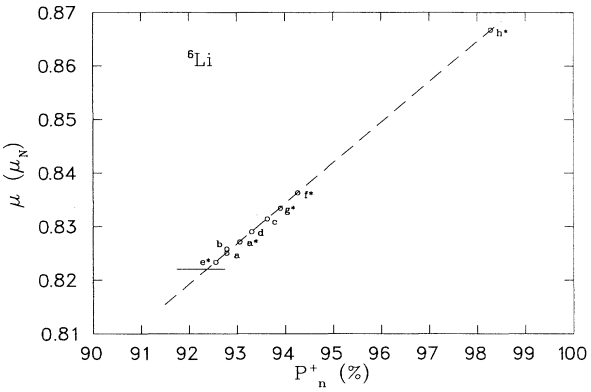

FIG. 3. Theoretical magnetic moments vs theoretical polarizations of the neutron in polarized ^{6}Li. The experimental moment $\mu = 0.822\,05$ nuclear magnetons is indicated as the horizontal line.

The quadrupole moment

So far, the results are very encouraging. Let us now turn to a well-known problem in three-body models of ^{6}Li: the sign of the quadrupole moment. As far as we know no dynamical three-body model has ever produced a negative value for Q, as is demanded by experiment. Could the experimental value be somehow wrong, or does this discrepancy point out a serious deficiency of the dynamical three-body model?

The experimental value of the quadrupole moment of ^{6}Li has changed since many of the phenomenological [10], resonating-group [9], and dynamical three-body model results were published. The new value is still very small and negative (indicating a slightly oblate nucleus with a primarily equatorial distribution of charge) but is now known to be about 30% more negative than the early value of -0.064 $e\,\mathrm{fm}^2$ still found in compilations and review articles. Quadrupole moments of nuclei are deduced from the experimental quadrupole coupling obtained from molecular resonance spectroscopy. From such experiments the quadrupole moment can only be extracted if a reliable theoretical value of the electric field gradient at the nucleus in the molecule is available. The experimental quadrupole coupling from the molecule ^{6}Li^{1}H can only be obtained with error bars of over 10%. Therefore one uses the ratio $Q(^6\mathrm{Li})/Q(^7\mathrm{Li})$ of $+0.0205(20)$ from experiments on LiF to deduce the value of $Q(^6\mathrm{Li})$ from the by now well-determined value of $Q(^7\mathrm{Li})$ [50]. A recent analysis of both molecular spec-

troscopy and Coulomb-scattering experiments reviews the last 20 years of effort and arrives at the consistent value of $Q(^7\mathrm{Li}) = -4.00 \pm 0.06\ e\,\mathrm{fm}^2$ [51]. Applying the ratio, one arrives at a value of $Q(^6\mathrm{Li}) = -0.082\ e\,\mathrm{fm}^2$ to compare with theoretical results.

This value is rather small when compared with $Q(\mathrm{D}) = +0.2860 \pm 0.0015\ e\,\mathrm{fm}^2$ [52] and explanations have been attempted in terms of αD cluster models. For an orientation to our results, we repeat the arguments of Ref. [9] which begin by mentioning that a two-cluster (αD) wave function with zero relative angular momentum would have no electric quadrupole moment and an additional d wave on the relative motion would give $Q(^6\mathrm{Li}) \simeq -1\ e\,\mathrm{fm}^2$. A three-cluster wave function, however, consisting of an alpha particle, a proton, and a neutron with s and d waves between them would have a positive Q because of the positive Q of the deuteron. An interplay between the s and d waves (l_y) between the clusters and within the deuteron (l_x) was found to account for the experimental $Q(^6\mathrm{Li})$ in a resonating-group calculation. (This is the same argument as those of Refs. [10], except that a deuteron with S and D waves is counted as a single cluster in those references.)

Turning now to our calculations (Table V), we find that none of the models has a negative value for the quadrupole moment, implying that all our models render a slightly prolate ^{6}Li. Since there are no adjustable parameters we must accept this. The present calculations seem to contradict the suggestion (made by Bang and Gignoux [33], as well as Kukulin *et al.* [44]) that the correct sign for Q can be obtained, just by taking a sufficient number of channels. The feeling that small wave-function components play a decisive role in the value of Q is justified (cf. Table IV), since $Q \propto \langle 3z^2 \rangle - \langle r^2 \rangle$ is a "difference" operator: its value is the result of a subtraction of two, almost equal, numbers. For a (nearly) spherical wave function we have that $\langle z^2 \rangle$ is nearly 1/3 times $\langle r^2 \rangle$, so that $Q/\langle r^2 \rangle \approx \langle 3(1/3)(r^2+\varepsilon) \rangle / \langle r^2 \rangle - 1 = \varepsilon / \langle r^2 \rangle \ll 1$. This makes Q extremely sensitive to small details in the wave function. As it turns out, however, the small wave components tend to make Q more positive and further away from experiment. Danilin *et al.* [37] suggest that the experimental value of Q for ^{6}Li may be evidence for an intrinsic polarization of the α particle in the field of a valence proton and would correspond to a quadrupole charge deformation parameter β_0 of the order of 10%. This refinement is outside of the scope of our model.

However, there is still room for improvement inside the three-body model. It must be noted that most αN model potentials fit low-energy data moderately well, and high-energy data not at all. One may argue that this is not very significant since it appears that the low-energy behavior is dominant in the ground state of ^{6}Li [38]. However, since Q is very sensitive to small details, we cannot ignore this shortcoming.

We have also found that the value of Q is sensitive to the angular-momentum structure of the αN interaction and the strength of the tensor force in the NN interaction. For example, the Malfliet-Tjon I-III NN potential with no tensor force predicts $Q(^6\mathrm{Li}_{\mathrm{TH}}) = +0.26\ e\,\mathrm{fm}^2$, even though the "deuteron" in the wave function has no D wave. Evidently, the interplay between the s and d waves (l_y) between the clusters and within the deuteron (l_x) demanded by potentials which fit the phase shifts is different from that which produces a negative value of Q. Another interesting case is model *f*. It is the only model that has a Majorana component in the αN interaction and it has a quadrupole moment which is significantly smaller than the other models (forgetting about models c, d, and h, which must be considered unrealistic). Unfortunately, model f fails to bind ^{6}Li sufficiently. This seems to be correlated to a rather poor fit to low-energy scattering data of this potential. In our opinion there is an urgent need for a truly energy-independent αN potential, which fits the scattering data over a large energy range. (Such a potential would have to be l dependent.)

The quadrupole moment may be a feature of ^{6}Li which is sensitive to an often neglected feature of dynamical three-body models and the defect may be cured by antisymmetrizing the wave function. Note that the three-body model is not fully antisymmetric, since exchange of nucleons inside the α particle with the valence nucleons has only approximately been treated. For example, an analysis of the charge form factor by Unkelbach and Hofmann [53] finds that both $C0$ and $C2$ contributions are very sensitive to the effects of antisymmetrization for their three-cluster wave functions. These authors use the resonating group method [54] and their wave functions are therefore fully antisymmetric with respect to an exchange of any two of the six nucleons. Upon full antisymmetrization $C2$ takes on the correct sign at low q and displays the unusual feature that the second maximum is larger than the first; both effects presumably due to cancellations of direct and exchange contributions generated by antisymmetrization.

It would appear, however, from another resonating-group calculation which included more angular-momentum channels [55], that the negative value of Q obtained in [9] might be a truncation artifact; this more recent RGM calculation finds $Q(^6\mathrm{Li}) = +0.25\ e\,\mathrm{fm}^2$, but Q becomes negative when they truncate to (almost) the model of Ref. [9]. A recent preprint by Kukulin *et al.* [56] with variational wave functions in a greatly expanded space displays a $C0$ unchanged by antisymmetrization and the minimum of $C2$ moved to slightly smaller q.

On the other hand, Hofmann finds that reducing the RGM model space does not change the sign of Q, but a separate calculation with a fully antisymmetrized wave function does give the correct sign [57]. We suggest that further work is needed to resolve this discrepancy and mention that the formalism needed to fully antisymmetrize the (converged) Faddeev wave functions of the dynamical three-body model is being developed [58].

Summary

To summarize the results of this subsection, we believe that the three-body model gives a quantitative description of ^{6}Li properties, except for the quadrupole moment. We therefore believe that it is justified to use this model as a starting point for the determination of polarization of the constituents.

B. Comparison with other results

In this subsection we ignore experiment and compare with other calculations within the same model. A theorist's concern is then (i) do the results accurately reflect the input potentials (issues of convergence, etc.), and (ii) how do the results depend on the input potentials. These questions were addressed in the previous section with regard to our calculations. In this subsection, we will concentrate on the results found in the literature in relation to our results. The data presented in Fig. 4, Table V, and Table VI will now be discussed with these questions in mind. Table VI presents a selection of the results found in the literature with different calculational methods (coordinate-space variational [32,45,59], coordinate-space direct solution of the Faddeev equations [33], hyperspherical expansion [37], and Faddeev integral equations in momentum space [38,48]) applied to a variety of input potentials.

Because the ^{6}Li radii of the variational calculations have already been noticed to be somewhat at odds with expectations from the binding energies [43], and because the wave functions of Ref. [60] have been used to analyze pion scattering from ^{6}Li [12], we attempted to reproduce the results Ref. [32]. As can be seen in Table VI (and in Fig. 4), a Faddeev calculation for model b with a RSC NN potential and SBB αN potential with (approximately) the same partial waves as those of [32,59], and finite suppression parameter Γ gives a binding energy about 2% smaller than our converged result and the full radius is 6% larger than the converged result. (This

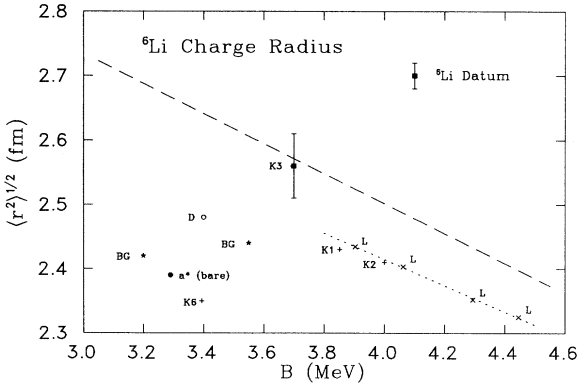

FIG. 4. The charge radius of ^{6}Li vs the binding energy B for breakup into α+n+p: comparison with other calculations. Variational results labeled "Ki", $i = 1, 2, 3, 6$, are taken from [32] ("K4" and "K5" have a binding energy less than 3 MeV), the Faddeev equation results of Bang and Gignoux labeled BG are taken from [33], the integral equation results labeled L are taken from [43], and the result from the hyperspherical expansion labeled D is from [37]. The Hamiltonian of "K6" (which corresponds to Kukulin-84 in Table VI) is the same as our model "$a^*_{\rm Kuk}$" of Table VI [plotted here as "a* (bare)"] and the approximate coincidence of the results implies that the radii of [32] plotted here are not charge radii but bare radii; see text for details. Note that K3 lies exactly on the experimental datum. Our results of Fig. 1 are not replotted here, but the straight line through our points is retained.

model is denoted by $a^*_{\rm Kuk}$ because the truncation of partial waves only allows $T = 0$ and therefore it has no isospin breaking.) It is somewhat surprising, then that the result of Ref. [32], listed as Kukulin-84, has a *full* charge radius which is 10% *smaller* than our converged result with this model. The explanation of this discrepancy may lie (as already noted in Ref. [43]) in the fact that the true wave function has, of course, the correct exponential falloff at large distances, and the Gaussian wave functions they utilize do not. However, the close agreement between $a^*_{\rm Kuk}$ and Kukulin-84 for both the energy and the (bare) radius, we think it is more likely that the radii listed in Table 1 of Ref. [32] are bare, although Kukulin claims to list full radii [61].

Continuing the comparison of Kukulin-84 and our model b truncated to $a^*_{\rm Kuk}$, we find that both models give a value of $Q \approx +0.2$. However, we find a much larger P-state probability for this model than the authors of [32] do. This probability, while not observable, does play a role in constituent polarizations, magnetic moments, and pion scattering as will be discussed shortly. Based on these comparisons, and the earlier discussion of longitudinal form factors and the charge radii, we believe that the wave functions from this early variational approach do not accurately reflect the input potentials. The same can be said for the results denoted by Kukulin-86 in Table VI, where both the P- and D-state probabilities appear to be too small. The variational results from a greatly expanded number of angular-momentum channels [45], labeled Kukulin-92 in Table VI, are another story. They are in reasonable agreement with our results for the same model b.

The other examples of calculations in Table VI are those of Bang and Gignoux [33], Danilin *et al.* [37], and Lehman *et al.* [43,48]. None of the inputs exactly match our models a–h, so the comparisons can only be qualitative. As mentioned in the discussion of our results, the convergence of the binding energy with the small number of channels used by Bang and Gignoux is not so bad and their wave-function results are in qualitative agreement with those of models e and g, the closest to their choice of potentials. The hyperspherical-expansion results [37] with yet another smooth NN potential (Gogny-Pires-de Toureil [62]) and the Sack potential are admitted to not have fully converged. But various methods are used to extrapolate to their asymptotic results in Table VI which are in qualitative agreement with those of Table V. The integral equations of [43,48] have to account only for mesh sizes and not a truncation of partial waves. This appears to be well under control as discussed in their papers and as shown by the nice straight-line fit in the radius-energy plane (cf. Fig. 4). As mentioned earlier, this is not as much as the case for the results from [32]. Especially the point $(B, r) = (3.393, 2.35)$, corresponding to Kukulin-84 and our model $a^*_{\rm Kuk}$, strikes us as odd. Most recently, their "final" result for this model (obtained with the RSC in all NN channels and a greatly expanded model space) is $(B, r) = (3.33, 2.44)$. Note also that one of the results of [32] lies above the αD breakup threshold, and therefore should not have a well-defined radius.

TABLE VI. Comparisons with other calculations.

Model	$\langle H\rangle$ (MeV)	$\langle r^2\rangle^{1/2}$ (fm)	$Q\,(e\,\mathrm{fm}^2)$	P_S (%)	P_P (%)	$P_{P'}$ (%)	P_D (%)
a^*_{Kuk}	−3.29	2.39[a]	+0.21	91.43	0	2.35	6.22
Kukulin-84 [32]	−3.39	2.35	+0.24	91.54	0	0.27	8.19
Kukulin-86 [59]	−3.85			95.54	0	1.08	3.38
Kukulin-92 [45]	−3.33	2.52	+0.40	90.16	0.15	2.12	7.55
b	−3.37	2.62	+0.59	89.48	0.22	2.65	7.65
Bang [33]	−3.20	2.44	pos.	92.8	0.7	5.3	1.2
Danilin [37]	~ -3.4	2.48	+0.40	93.04	0.24	3.34	3.38
Proj. (4%) [43,48]	−3.90	2.43		91.47	0.48	4.65	3.40
Rep. (4%) [43,48]	−4.06	2.40		91.78	0.50	4.01	3.71

[a]This is the *bare* radius, i.e., without taking into account the electromagnetic size of the constituents. We believe that it is this radius which should be compared to that labeled Kukulin-84. The full radius (i.e., the radius one gets if the electromagnetic size of the constituents is taken into account) is 2.79 fm. Note that some authors give matter radii instead on charge radii. These two quantities are identical if the $T = 1$ component of the wave function is ignored, and the constituent charge radii are taken to be equal to the constituent matter radii.

After checking on the reliability of the results a theorist turns to the question of how the output depends on the input. The most systematic attempt to answer this second question is found in the program of Lehman and collaborators who fit five different separable potentials to the *same* low-energy NN and αN data. Each set of potentials addresses a specific question such as the strength of the tensor force in the NN interaction (labeled by 0% or 4% D state in the deuteron as shown in Table VI) or whether the s-wave αN interaction does support a state forbidden by the Pauli potential that must be projected out ("proj.") or does not ("rep."). In our opinion, the drawback of these potentials is that they do not contain a short-range repulsion, they do not include the negative-parity terms of the NN interaction, and they are separable and the nonlocality is hard to relate to an underlying meson-exchange picture. Finally, the Coulomb force cannot be included in the model. Thus we feel that there is room for further studies such as ours.

One aspect of the dependence of the three-body model results upon the input which has entered into the folklore has to do with the wave-function probability $P_{P'}$. It is stated in its purest form in a recent publication [55]: "It is plausible and has been corroborated by test calculations that the weight of this contribution depends crucially and almost solely on the singlet odd $^1P_1$ term of the nucleon-nucleon force [. . .]." This assertion perhaps stems from the statement in [32] that the value of $P_{P'} = \beta^2 \ll 1\%$ was due to the repulsive NN interaction in the P wave: "If the NN interaction in the P wave is excluded, the value of β will rise." However, a better numerical treatment of the RSC potential soon raised $P_{P'}$ from 0.27% in [32] to the 1.08% quoted in [59] and Table VI and eventually a large expansion of the angular-momentum channels lead to the 2.12% of the "final" solution Kukulin-92 [45] displayed in Table VI. The results in Kukulin-92 are in reasonable agreement with our results for the same model but P-state probabilities are still somewhat smaller than the other calculations. Now we return to the relation between $P_{P'}$ and the NN interaction in the $^1P_1$ channel. It is well known that the $^1P_1$ phase shifts of the RSC potential are about half the size of experiment, because Reid fitted his potential to phase shift solutions from data which have since been discarded [63,64]. Perhaps we should be concerned because we used a bad NN potential for models a–f. Perhaps, but not for this reason. Notice that in Table VII the probability $P_{P'}$ in ^{6}Li varies by a factor of 6 for the same RSC NN potential and different αN potentials, whereas it hardly changes when RSC (model a) is replaced by SSC (model g) which has better $^1P_1$ phase shifts. That is, our results do not support this bit of ^{6}Li folklore.

VII. NUCLEON POLARIZATION IN $^6\vec{\mathrm{Li}}$

The predictions of the polarization of the neutron, expressed as a percentage of the fully polarized $^6\vec{\mathrm{Li}}$, have

TABLE VII. Probabilities in eight different systems.

Model	P_S (%)	P_P (%)	$P_{P'}$ (%)	P_D (%)	$P_n^+[/P_p^+]$ (%)	$\mu(\mu_N)$
a	89.290(2)	0.232(2)	2.808(4)	7.667(2)	92.788(1)	0.82502(3)
a*	89.590(1)	0.647(1)	2.166(4)	7.596(2)	93.057(1)	0.82708(3)
b	89.478(2)	0.223(4)	2.647(3)	7.650(3)	92.796(3)/92.982(2)	0.82575(3)
c	90.626(1)	0.216(1)	2.861(1)	6.519(1)	93.626(1)	0.83139(2)
d	90.163(1)	0.206(1)	2.341(1)	7.291(1)	93.310(1)	0.82899(2)
e*	88.712(2)	0.441(1)	3.218(1)	7.630(3)	92.559(2)	0.82328(2)
f*	92.119(5)	0.105(1)	0.536(1)	7.239(3)	94.275(4)	0.83633(2)
g*	90.881(1)	0.237(1)	2.463(3)	6.418(1)	93.896(1)	0.83344(2)
h*	96.573(1)	0.197(1)	2.995(1)	0.236(1)	98.277(1)	0.86671(2)

already been displayed in Table V. In this table, the calculated polarizations are greater than 90% for the valence nucleons in the three-body model of ^{6}Li, close to an estimate of 97% obtained from the two-body model of ^{6}Li with the aid of (14). However, the overlap of the three-body wave function on the "α+D" structure gives a probability of 60–70 % for most models so the naive guess from the two-body model of ^{6}Li must be scaled down to about 58–68 %. It is remarkable that the "uncorrelated" valence nucleons of the part of the wave function which is not "α+D" in the exact calculation boost this back up to $P_n^+ \geq 90\%$. In Table VII we give the probabilities of the wave-function components and the calculated value of P_n^+ for our models. Note that the proton polarizability is marginally larger than the neutron polarizability for model b, the only model which has a $T = 1$ component. For the other models there is just one polarizability, since the proton and neutron are considered identical. It is clear from (16) that $P_n^+ \geq P_S$ and that the exact value of the neutron polarization depends on the smaller probabilities of the P and D states. Since these are well defined within a model but are not observables [17,18], polarization predictions of models of ^{6}Li should be tested by knockout reactions [8,13], scattering by polarized proton beams [14], and other experimental probes. That is, a program for ^{6}Li similar to the program which tests the ^{3}He wave function by knockout reactions [15], scattering by polarized proton beams [16], etc., would, in our opinion, be helpful to test our predictions.

In the absence of such a program, we can use the fact that the magnetic moment for the ground state of ^{6}Li can also be written in terms of these probabilities, as discussed in the previous section, to help calibrate our polarization estimates. Observing as we did earlier that models a and b which have binding energies, longitudinal form factors, and charge radii in excellent agreement with experiment also predict a magnetic moment within 1% of the experimental value of 0.822 05 nuclear magnetons, we feel there is strong support to the polarization prediction of 93% from these models.

The magnetic moment is the zero momentum transfer limit of the transverse form factor. This form factor has been invoked in attempt to understand the angular distribution of the vector analyzing power iT_{11} for π^+-$^6\vec{\text{Li}}$ elastic and inelastic scattering. The argument goes as follows. "The transversal form factor F_T is expected to be very close to (the pion-nuclear spin form factor) $F_{el}^S(q)$ because the convection current contribution almost vanishes in e-^{6}Li scattering, if $L = 0$ is really the dominating configuration in the ^{6}Li ground-state wave function" [12]. This statement can be quantified at the $q \to 0$ limit by the explicit formula for the orbital contribution μ_L to the magnetic moment [48]

$$\mu_L = \tfrac{1}{2}[\tfrac{1}{2}P_P + P_{P'} + \tfrac{3}{2}P_D]\,. \tag{36}$$

Typical values from Table VII suggest that the orbital motion contributes ~ 0.05 to the total moment of ~ 0.83. In the existing treatments of pion-nucleus scattering, the details of the pion-nucleon interaction are subsumed into this spin form factor $F_{el}^S(q)$ whose shape is determined by the underlying nuclear wave function. The analysis of [12] finds that a shell-model wave function describes the data marginally better than one of the earliest variational three-body wave functions of Kukulin *et al.* [60]. Our probabilities of the P- and D-state components from Table VII (typically $P_{P'} \approx 2$–$3\,\%$, $P_P \approx 0.2$–$0.6\,\%$, $P_D \approx 6.5$–$6.7\,\%$) are quite different from those of the wave function [60] ($P_{P'} \leq 0.5\%$, $P_P = 0.0$, $P_D = 0.0$) used in [12]. The spin form factor from any of the wave functions of our models is quite likely to be different from the three-body model already used. At present we can only speculate on the changes which might occur if one of our wave functions (or indeed one from Ref. [45]) were used to analyze the pion scattering data. A new calculation of the angular distribution of the vector analyzing power iT_{11} for π^+-$^6\vec{\text{Li}}$ elastic and inelastic scattering would seem to be in order before one could conclude finally that the three-body model of ^{6}Li cannot explain this data as well.

VIII. SUMMARY AND OUTLOOK

We have solved the configuration-space Faddeev equations of the dynamical three-body model which characterizes ^{6}Li as a bound system of an alpha particle, a neutron, and a proton interacting with local potentials which parametrize the free-space forces between the three particles. We have made an exhaustive study of the convergence of our solutions both in the spline approximation and in the number of partial waves (channels) kept in the angular-momentum expansion of the Faddeev amplitudes. Our observables (and wave-function expectation values) are the result of extrapolation to infinite grid size and an infinite number of channels, i.e., they are absolute predictions of the model. For this reason, we were able to compare with earlier solutions, which did not include so many channels, to draw conclusions about the quality of the concomitant wave functions.

Most of our models used the Reid soft core NN potential with a variety of αN potentials which more or less fit the low-energy αN phase shifts. We could estimate the effect of the Coulomb potential perturbatively or could include it in the full Hamiltonian and found that perturbation theory works very well. Futhermore, the Coulomb potential has a tiny effect on all expectation values except the binding energy and the charge radius. All the models assumed a pure $T = 0$ state for ^{6}Li except one (labeled b) which checked this simplification by including explicit isospin breaking generated by the Coulomb potential and the neutron-proton mass difference. Isospin breaking increased the binding energy by about 4%. Most αN potentials support s-wave states in the five-nucleon system which are forbidden by the Pauli principle. These Pauli-forbidden states are projected out exactly using a new equation for the Faddeev amplitude which we have shown to be the limit of the traditional pseudopotential approach used to deal with forbidden-state potentials [20,32].

Comparison of observables of our converged calcula-

tions with the experimental properties of the ground state of ^{6}Li was quite satisfying. For 13 models a plot of charge radius vs binding energy (Fig. 1) displays points which scatter around a straight line which passes through the experimental datum. Our most sophisticated models a* and b (RSC NN potential, a Gaussian potential by Sack *et al.* which fits s- and p-wave phase shifts of the αN interaction, and the Coulomb interaction without and with isospin breaking) are within 10% of the experimental binding energy and within the error bars of the charge radius. The experimental longitudinal form factor is described well up to momentum transfer $q = 2.5$ fm^{-1}. The magnetic moment is described well by most of the models and extremely well by the models which are near the radius-binding energy datum. The very small quadrupole moment is not described well by our calculations, nor by any calculation in the dynamical three-body model of ^{6}Li. The explanation of this discrepancy may well lie outside this model.

Our motivation for undertaking these calculations was to examine, within a well-defined and controlled model, the extent that the nucleons in $^6\vec{\text{Li}}$ are themselves spin aligned and could therefore be considered polarized targets for measurements of the spin structure function of the neutron and proton. It is, of course, the polarized neutron which is the desired target because it can only be utilized when bound in a nucleus. $^6\vec{\text{Li}}$ has been suggested as a target for the study of direct photon production with polarized proton beams and polarized nucleon targets which could determine the spin-dependent gluon distribution in the nucleon [2]. This information on the uncharged constituents of the nucleon is needed to complement the knowledge of the spin-dependent quark and antiquark distributions obtained from deep-inelastic scattering of longitudinally polarized leptons from longitudinally polarized nuclei. The first results from lepton scattering on the spin-dependent structure function $g_1(x)$ of the deuteron have been published [65], and those from ^{3}He have been announced [66]. To infer from this data the first moment of the spin-dependent neutron structure function (for a comparison with sum rules), one needs to know the polarization of the nucleons within the polarized nucleus. Our Eq. (14) for the deuteron and similar formulas for ^{3}He [11] provide this information theoretically. In this paper we have developed the formulas and done the calculation for the polarization of the valence nucleons of the three-body model of ^{6}Li. We find a polarization of the neutrons in excess of 30% of the $^6\vec{\text{Li}}$. This theoretical result implies that ^{6}LiD should provide a very good target of polarized neutrons (45%) for the hadronic experiments to determine the polarized gluon distribution of the nucleon.

Our result is couched as the answer to the question "If we pick a nucleon from the fully polarized nucleus without disturbing its spin, what is the degree of polarization of that spin?" This question is a theorist's question and may or may not be answerable in a given experiment. Indeed, we have not seen a discussion of this point in the few published results of polarized lepton scattering and wish to reiterate the necessity of testing such predictions before extracting *neutron* spin-dependent structure functions from measurements on nuclei. For example, the HERMES experiment will measure the spin-dependent structure functions of hydrogen, deuterium, and ^{3}He in one series of measurements [4]. In addition, there is a vigorous experimental program to support the deep-inelastic scattering measurements which tests the ^{3}He wave function by knockout reactions [15], scattering by polarized proton beams [16], etc. In our opinion, no less a commitment should be made to the interpretation of the proposed direct photon production experiments at Fermilab [2]. That is, our polarization predictions of models of ^{6}Li should be tested by knockout reactions [8,13], scattering by polarized proton beams [14], and other experimental probes.

ACKNOWLEDGMENTS

This project began when SAC and NWS came together at the Institute for Nuclear Theory of the University of Washington. We wish to thank the Institute Director Ernest Henley and Program Director Jim Friar for creating a stimulating and productive atmosphere at the Institute. It was also supported in part by National Science Foundation Grant PHY-9017058. N.W.S. wishes to thank the physics department of New Mexico State University for hospitality and, in particular, the geophysics group for generously providing computer support during a short visit. S.A.C. acknowledges stimulating and helpful discussions with Ana Eiró, Antonio Fonseca, Teresa Peña, Shirley Cooper, Ray Mackintosh, Ron Johnson, George Burleson, Gary Kyle, and the members of his nuclear theory class at NMSU. We have benefited from e-mail discussions with Hartmut Hartmann and V. I. Kukulin and from the receipt of preprints from the latter. R.M.A. would like to thank FOM (Fundamenteel Onderzoek der Materie) for financial support and Ben Bakker for useful discussions.

[1] P. Chaumette, J. Deregal, G. Durand, and J. Fabre, in *Future Polarization Physics at Fermilab*, Proceedings of the Symposium, Batavia, IL, 1988, edited by E. Berger, J.G. Morfin, A.L. Read, and A. Yokosawa (Fermilab, Batavia, 1988), p. 257; see also G. Chaumette, J. Deregel, G. Durand, J. Fabre, and L. van Rossum, in *High Energy Spin Physics, Eighth International Symposium*, Proceedings of the Eighth International Symposium Held on High-Energy Spin Physics: Eighth International Symposium at the University of Minnesota, 1988, AIP Conf. Proceedings No. 187, edited by K.J. Heller (AIP, New York, 1989), Vol. 2, p. 1275.

[2] Fermilab proposal No. 809, A. Masaike, S. Nurushev, and A. Yokosawa, spokepersons, 1990 (unpublished).

[3] J. Ashman *et al.*, European Muon Collaboration, Phys. Lett. B **206**, 364 (1988).

[4] HERMES Collaboration Report No. DESY-PRC-90-01, 1990 (unpublished).

[5] E.L. Berger and J. Qiu, Phys. Rev. D **40**, 3128 (1989).
[6] D.R. Lehman and Mamta Rajan, Phys. Rev. C **25**, 2743 (1982).
[7] D.R. Lehman and W.C. Parke, Phys. Rev. C **28**, 364 (1983).
[8] J.B.J.M. Lanen *et al.*, Phys. Rev. Lett. **62**, 1925 (1989).
[9] T. Mertelmeier and H.M. Hofmann, Nucl. Phys. **A459**, 387 (1986).
[10] H. Nishioka, J.A. Tostevin, and R.C. Johnson, Phys. Lett. **124B**, 17 (1983); A.C. Merchant and N. Rowley, *ibid.* **150B**, 35 (1985).
[11] J.L. Friar, B.F. Gibson, G.L. Payne, A.M. Bernstein, and T.E. Chupp, Phys. Rev. C **42**, 2310 (1990).
[12] S. Ritt *et al.*, Phys. Rev. C **43**, 754 (1991).
[13] LAMPF proposal No. 1204, A. Klein and K.-M. Koch, spokespersons, 1990 (unpublished).
[14] LAMPF proposal No. 1206, G.W. Hoffmann, K.-M. Koch, and B. Burleson, spokespersons, 1990 (unpublished).
[15] A. Rahav *et al.*, Phys. Rev. C **46**, 1167 (1992); Phys. Lett. B **275**, 259 (1991).
[16] K. Lee *et al.*, CE-25 Collaboration, Bates Report B/IR 92-06 (submitted to Phys. Rev. Lett.).
[17] R. Amado, Phys. Rev. C **19**, 1473 (1979).
[18] J.L. Friar, Phys. Rev. C **20**, 325 (1979).
[19] N.W. Schellingerhout, L.P. Kok, and G.D. Bosveld, Phys. Rev. A **40**, 5568 (1989).
[20] D.R. Lehman, Phys. Rev. C **25**, 3146 (1982); W.C. Parke and D.R. Lehman, *ibid.* **29**, 2319 (1984).
[21] D.R. Lehman, *Few-Body Systems and Multiparticle Dynamics*, Proceedings of the Symposia of the Topical Group on Few-Body Systems and Multiparticle Dynamics, AIP Conf. Proceedings No. 162, edited by D.A. Micha (AIP, New York, 1987), p. 131.
[22] D. Baye, Phys. Rev. Lett. **58**, 2738 (1987).
[23] C.V. Sukumar, J. Phys. A **18**, 2917 (1985); **18**, 2937 (1985).
[24] E. Witten, Nucl. Phys. **B188**, 513 (1981).
[25] R.D. Amado, F. Cannata, and J.P. DeDonder, Phys. Rev. C **41**, 1289 (1990).
[26] R.V. Reid Jr., Ann. Phys. (N.Y.) **50**, 411 (1968); B.D. Day, Phys. Rev. C **24**, 1203 (1981).
[27] R. de Tourreil and D.W.L. Sprung, Nucl. Phys. **A201**, 193 (1973).
[28] R.A. Malfliet and J.A. Tjon, Ann. Phys. (N.Y.) **61**, 425 (1970).
[29] S. Sack, L.C. Biedenharn, and G. Breit, Phys. Rev. **93**, 321 (1954).
[30] G.R. Satchler, L.W. Owen, A.J. Elwyn, G.L. Morgan, and R.L. Walter, Nucl. Phys. **A112**, 1 (1968).
[31] S.G. Cooper and R.S. Mackintosh, Phys. Rev. C **43**, 1001 (1991).
[32] V.I. Kukulin, V.M. Krasnopol'sky, V.T. Voronchev, and P.B. Saznov, Nucl. Phys. **A417**, 128 (1984).
[33] J. Bang and C. Gignoux, Nucl. Phys. **A313**, 119 (1979).
[34] S. Ali, A.A.Z. Ahmad, and N. Ferdous, Rev. Mod. Phys. **57**, 923 (1985).
[35] C.M. Perey and F.G. Perey, At. Nucl. Data Tables **17**, 1 (1976).
[36] J.M. Bang, I.J. Thompson, M.V. Zhukov, B.V. Danilin, D.V. Fedorov, and J.S. Vaagen, Niels Bohr Institute Report NBI-91-31, 1991.
[37] B.V. Danilin, M.V. Zhukov, A.A. Korsheninnikov, and L.V. Chulkov, Yad. Fiz. **53**, 71 (1991) [Sov. J. Nucl. Phys. **53**, 45 (1991)].
[38] D.R. Lehman, M. Rai, and A. Ghovanlou, Phys. Rev. C **17**, 744 (1978).
[39] R.A. Arndt, D.D. Long, and L.D. Roper, Nucl. Phys. **A209**, 429 (1973).
[40] G. Höhler, E. Pietarinen, I. Sabba-Stefanescu, F. Borkowsky, G.G. Simon, V.H. Walther, and R.D. Wendling, Nucl. Phys. **B114**, 505 (1976).
[41] I. Sick, J.S. McCarthy, and R.R. Whitney, Phys. Lett. **64B**, 33 (1976); I. Sick, private communication.
[42] G.C. Li, I. Sick, R.R. Whitney, and M.R. Yearian, Nucl. Phys. **A162**, 583 (1971).
[43] A. Eskandarian, D.R. Lehman, and W.C. Parke, Phys. Rev. C **38**, 2341 (1988).
[44] V.I. Kukulin, V.T. Voronchev, T.D. Kaipov, and R.A. Eramzhyan, Nucl. Phys. **A517**, 221 (1990).
[45] V.I. Kukulin, V.N. Pomerantsev, Kh.D. Rasikov, V.T. Voronchev, and G.G. Ryzhikh, Australian National University Report ANU-ThP-1/92, 1992.
[46] S. Klarsfeld, J. Martorell, and D.W.L. Sprung, J. Phys. B **10**, 165 (1984). See M. Kohno, *ibid.* **9**, L85 (1984) for further discussion.
[47] R. Schiavilla and D.O. Riska, Phys. Rev. C **43**, 437 (1991).
[48] D.R. Lehman and W.C. Parke, Few-Body Systems **1**, 193 (1986).
[49] J.L. Friar, Phys. Rev. C **27**, 2078 (1983); for a discussion of mesonic exchange contributions to the magnetic moment of the isoscalar deuteron see J.L. Friar, in *Mesons in Nuclei*, edited by M. Rho and D.H. Wilkinson (North-Holland, Amsterdam, 1979), p. 597, and [18].
[50] D. Sundholm, P. Pyykkö, L. Laaksonen, and A.J. Sadlej, Chem. Phys. Lett. **112**, 1 (1984).
[51] H.-G. Voelk and D. Fick, Nucl. Phys. **A530**, 475 (1991).
[52] D.M. Bishop and L.M. Cheung, Phys. Rev. A **20**, 381 (1979).
[53] M. Unkelbach and H.M. Hofmann, Few-Body Systems **11**, 143 (1991).
[54] H.H. Hackenbroich, Z. Phys. **231**, 216 (1970); **231**, 225 (1970); H.M. Hofmann, in *Models and Methods in Few-Body Physics, Proceedings Lisboa, Portugal, 1986*, edited by L.S. Ferreira, A.C. Fonseca, and L. Streit, Lecture Notes in Physics Vol. 273 (Springer-Verlag, Berlin, 1987), p. 241.
[55] A. Csótó and R.G. Lovas, Phys. Rev. C **46**, 576 (1992).
[56] G.G. Ryzhikh, R.A. Eramzhyan, V.I. Kukulin, and Yu.M. Tchuvil'sky (unpublished).
[57] H. Hartmann, private communication.
[58] B.L.G. Bakker and R.M. Adam, private communication.
[59] V.I. Kukulin, V.M. Krasnopol'sky, V.T. Voronchev, and P.B. Saznov, Nucl. Phys. **A453**, 365 (1986).
[60] V.M. Krasnopol'sky, V.I. Kukulin, P.B. Saznov, and V.T. Voronchev, Phys. Lett. **121B**, 96 (1983).
[61] V.I. Kukulin, private communication.
[62] D. Gogny, P. Pires, and R. de Tourreil, Phys. Lett. **32B**, 591 (1970).
[63] F.P. Brady, *Few Body Systems and Nuclear Forces*, edited by H. Zingl, M. Haftel, and H. Zankel, Lecture Notes in Physics Vol. 82 (Springer-Verlag, Berlin, 1978), p. 137.
[64] The current NN phase shifts can be obtained interactively through the Scattering Analysis Interactive Dial-In (SAID) program at VPI.
[65] B. Adeva *et al.*, Phys. Lett. B **302**, 533 (1993).
[66] P. Souder, unpublished.